

A Subdivision Scheme for Continuous-Scale B-Splines and Affine-Invariant Progressive Smoothing

GUILLERMO SAPIRO

Hewlett-Packard Labs, 1501 Page Mill Rd., Palo Alto, CA 94304

ALBERT COHEN

Laboratoire d'Analyse Numerique, Université Pierre et Marie Curie, 4 Place Jussieu, Paris 75005, France

ALFRED M. BRUCKSTEIN

Department of Computer Science, Technion-Israel Institute of Technology, Haifa 32000, Israel

Abstract. Multiscale representations and progressive smoothing constitute an important topic in different fields as computer vision, CAGD, and image processing. In this work, a multiscale representation of planar shapes is first described. The approach is based on computing classical B-splines of increasing orders, and therefore is automatically affine invariant. The resulting representation satisfies basic scale-space properties at least in a qualitative form, and is simple to implement.

The representation obtained in this way is discrete in scale, since classical B-splines are functions in \mathbf{C}^{k-2} , where k is an integer bigger or equal than two. We present a subdivision scheme for the computation of B-splines of finite support at continuous scales. With this scheme, B-splines representations in \mathbf{C}^r are obtained for any real r in $[0, \infty)$, and the multiscale representation is extended to continuous scale.

The proposed progressive smoothing receives a discrete set of points as initial shape, while the smoothed curves are represented by continuous (analytical) functions, allowing a straightforward computation of geometric characteristics of the shape.

Keywords: B-spline representations, subdivision schemes, continuous scale, affine invariant, progressive smoothing, computer implementation

1. Introduction

Multiscale descriptions of signals have been studied for several years already since Witkin's work [43], and developed in several different frameworks by a number of researchers in the past decade [4, 8, 14, 17, 21, 25–27, 30–32, 34, 44]. The idea of scale-space filtering is based on filtering a given initial signal $\Phi_0(\vec{X}) : \mathbb{R}^n \rightarrow \mathbb{R}^m$ with a family of filters $\mathcal{K}(\vec{X}, t) : \mathbb{R}^n \rightarrow \mathbb{R}^m$, where $t \in \mathbb{R}^+$ represents the scale. In other words, the scale-space is given by $\Phi(\vec{X}, t)$ defined as

$$\Phi(\vec{X}, t) := \Omega_{\mathcal{K}(\vec{X}, t)}[\Phi_0(\vec{X})], \quad (1)$$

where $\Omega_{\mathcal{K}(\cdot, t)}[\cdot]$ represents the action of the filter $\mathcal{K}(\cdot, t)$. Larger values of t correspond to signals at coarser resolutions.

A classical example of a scale-space kernel is the Gaussian one. In this case, the scale-space is linear, and the filter in (1) is defined via convolution. The Gaussian kernel is one of the most studied in the theory of scale-spaces [4, 21, 25, 44]. It has some very interesting properties, one of them being that the signal Φ obtained from it is the solution of the heat equation (with Φ_0 as initial condition) given by

$$\frac{\partial \Phi}{\partial t} = \Delta \Phi.$$

One of the key facts that can be gleaned from the Gaussian example is that the scale-space can be obtained as the solution of a partial differential equation called an *evolution equation*. This idea was developed in different works [1–3, 23, 24, 38] for evolution equations different from the classical heat flow.

Let's concentrate now on the family of planar curves

$$C(u, t) : [a, b] \times [0, \tau] \rightarrow \mathbb{R}^2,$$

and define the evolution equation

$$\begin{cases} \frac{\partial C}{\partial t} = \frac{\partial^2 C}{\partial p^2}, \\ C(u, 0) = C_0(u). \end{cases} \quad (2)$$

If $p \equiv u$, then the classical heat equation is obtained. If $p \equiv v$, where v is the *Euclidean arc-length* [42], the *Euclidean shortening flow*, or *Euclidean geometric heat flow*, is obtained [18, 20]. This equation defines a geometric Euclidean invariant scale-space [2, 24, 32]. If $p \equiv s$, where s is the *affine arc-length* [6], then the *affine shortening flow*, or *affine geometric heat flow*, is obtained [36, 37]. Sapiro and Tannenbaum [36, 37, 39] proved that this equation is the affine analog of the Euclidean shortening flow, and that any simple curve converges to an ellipse when evolving according to it (in the Euclidean case, convergence to a circle is obtained [18, 20]). The affine flow was implemented using an efficient numerical algorithm for curve evolution presented in [33], and based on this, a geometric affine invariant scale-space for planar curves was defined [38].

In general, a number of properties are required to form a scale-space [1, 4]. Some of the basic properties are:

1. *Completeness*. The original signal should be obtained when $t \rightarrow 0$.
2. *Order preserving*. If $\Phi_0 < \bar{\Phi}_0$, then $\Phi(t) < \bar{\Phi}(t)$ for all $t > 0$. This property is violated for example for 2D Gaussian filters (shapes can merge).
3. *Causality criterion*. This criterion means that “information” is not added when moving from a finer to a coarser scale. The “information” can be characterized for example by zero-crossings¹, extrema, total curvature, and so on. The causality criterion is usually also related to the *semi-group property* (specially when the scale-space is derived from evolution equations): The signal $\Phi(\bar{X}, t_2)$ (see

Eq. (1)) can be obtained either from the initial signal $\Phi(\bar{X}, 0)$ via $\Omega(t_2)$, or from an intermediate one $\Phi(\bar{X}, t_1)$ via $\Omega(t_2 - t_1)$ ($t_1 < t_2$).

In [1], Alvarez et al. gave a characterization of the evolution equations for which these and other properties hold. Examples are, of course, both the classical and the geometric heat flows described above [1, 2, 38].

The multiscale representation here developed is not obtained as the solution of an evolution equation. It is based on computing B-spline representations at different orders. Increasing the order of the B-spline representation, smoother curves are obtained. Therefore, the B-spline order plays the role of the scale parameter in previously described scale-spaces. We will show that the above mentioned multiscale representation properties hold at least in a qualitative form. Since B-splines are affine-invariant, so is the obtained representation. This means that the B-spline representations of two series of control points related by an affine motion, are related by the same affine motion.

Classical B-splines are functions in \mathbf{C}^{k-2} , where k , the B-spline order, is an integer number bigger or equal than 2. Therefore, the multiscale representation based on classical B-splines of different orders, is discrete in its “scale” parameter k .² Based on subdivision schemes, we present an extension of the classical B-spline basis in order to obtain a finite support basis in \mathbf{C}^r , $r \in [0, \infty)$. This way, we also obtain a continuous in “scale” multiscale B-spline based representation.

The proposed B-spline based progressive smoothing (representation) is easy to implement (see Sections 2 and 4). In contrast with frequently used scale-spaces, as the Gaussian one, it is defined directly (intrinsically) on an initial discrete set of points, avoiding possible problems caused by discretization of continuous scale-spaces. See for example [30] for an analysis of this problem in linear scale-spaces, and a possible solution. (Related to this see also [17].) While the initial signal is discrete, the smoothed one is continuous and defined as a linear combination of B-spline basis. This allows a straightforward computation of geometric properties of the smoothed curve, as for example curvature or other invariants [22]. With the continuous scale B-spline basis presented in this paper, the representation is continuous in scale as well. Therefore, the proposed representation is natural for computer shape analysis, since it receives as input a digital signal, while keeping a continuous representation which can be helpful for different computations.

The remainder of this paper is organized as follows: Section 2 gives a brief description of the theory of B-spline approximations. Section 3 presents the affine invariant multiscale representation based on classical B-splines basis. The continuous scale B-spline basis, developed using subdivision schemes, is presented in Section 4. Concluding remarks are given in Section 5.

2. Basic Concepts on B-Splines

We briefly describe now the theory of B-spline approximations. For details see for example [5, 9, 40, 41].

Let

$$\mathcal{C}(u) : [a, b] \rightarrow \mathbb{R}^2$$

be a planar curve, with Cartesian coordinates $[x(u), y(u)]$. Polynomials are computationally efficient to work with, but it is not always possible to define a satisfactory curve \mathcal{C} using single polynomials for x and y . Then, the curve is divided in segments, each one defined by a given polynomial. The segments are joined together to form a *piecewise polynomial* curve. The joints between the polynomial segments occur at special curve points called *knots*. The sequence u_1, u_2, \dots of knots is required to be nondecreasing. The distance between two consecutive knots can be constant or not. Two successive polynomial segments are joined together at a given knot u_j in such a way that the resulting piecewise polynomial has d continuous derivatives. Of course, the order of the polynomials depends on d . In this way, a basis is obtained, and the curve \mathcal{C} is given by a linear combination of it.

Formally, the curve \mathcal{C} is a *B-spline* approximation of the series of points $V_i = [x_i, y_i]$, $1 \leq i \leq n$, called *control vertices*, if it can be written as

$$\mathcal{C}_k(u) = \sum_i^n V_i B_{i,k}, \quad (3)$$

where $B_{i,k} = B(\cdot; u_i, u_{i+1}, \dots, u_{i+k})$ is the i -th *B-spline basis* of order k for the knot sequence $[u_1, \dots, u_{n+k}]$. In particular, $B_{i,k}$ is a piecewise polynomial function of degree $< k$, with breakpoints, u_i, \dots, u_{i+k} .³

Several properties can be proven for the basis $B_{i,k}$:

1. $B_{i,k} \geq 0$.
2. $B_{i,k} \equiv 0$ outside the interval $[u_i, u_{i+k}]$. This property shows the locality of the approximation:

Changing a given control vertex affects only a corresponding portion of the curve.

3. The basis is normalized for all order k :

$$\sum_i B_{i,k}(u) = 1 \quad \text{on } [u_k \cdots u_{n+1}].$$

4. The support of the B-spline basis is minimal among all polynomial splines of order k . This property shows that this representation is optimal in certain sense.

The multiplicity of the knots governs the smoothness. If a given number τ occurs r times in the knot sequence $[u_i, \dots, u_{i+k}]$, then the first $k - r - 1$ derivatives of $B_{j,k}$ are continuous at the breakpoint τ . Therefore, without knot multiplicity, $\mathcal{C}_k \in \mathbf{C}^{k-2}$.

Computation with B-splines are facilitated by using the following recursive formula [5, 9, 10]:

$$B_{i,k}(u) = \frac{u - u_i}{u_{i+k-1} - u_i} B_{i,k-1} + \frac{u_{i+k} - u}{u_{i+k} - u_{i+1}} B_{i+1,k-1}, \quad (4)$$

together with

$$B_{i,1}(u) = \begin{cases} 1 & u_i \leq u < u_{i+1}, \\ 0 & \text{otherwise.} \end{cases} \quad (5)$$

The basis $B_{i,k}$ is in fact the repeated convolution of a Haar function with itself, i.e.,

$$B_{0,k} = (*)^k \chi[0, 1].$$

3. The B-Spline Multiscale Representation

A general *affine* transformation in the plane (\mathbb{R}^2) is defined as

$$\tilde{X} = AX + T, \quad (6)$$

where $X \in \mathbb{R}^2$ is a vector, $A \in \text{GL}_2^+(\mathbb{R})$ (the group of invertible real 2×2 matrices with positive determinant) is the affine matrix, and $T \in \mathbb{R}^2$ is a translation vector. It is easy to show that transformations (A, T) of the type (6) form a real algebraic group \mathcal{A} , called the *group of proper affine motions*. If $A \in \text{SL}_2(\mathbb{R})$ (i.e, the determinant of A is 1), (6) gives the *group of special affine motions*, \mathcal{A}_{sp} .

A quantity Q is called an *invariant* of the group \mathcal{A} if whenever Q transforms into \tilde{Q} by any transformation

$(A, T) \in \mathcal{A}$, we obtain $\tilde{Q} = \Psi Q$, where Ψ is a function of (A, T) alone. If $\Psi \equiv 1$ for all $(A, T) \in \mathcal{A}$, Q is called an *absolute invariant* [13].

Observe that from (3), the affine invariant property of the B-spline representation is immediate. If $\{\tilde{V}_i\}_1^n$ is obtained from $\{V_i\}_1^n$ by an affine transformation (A, T) , then

$$\tilde{C}_k(u) = AC_k(u) + T, \quad (7)$$

where

$$C_k(u) = \sum_i^n V_i B_{i,k},$$

and

$$\tilde{C}_k(u) = \sum_i^n \tilde{V}_i B_{i,k}.$$

Note that the representation is invariant with respect to affine transformations of the control points $\{V_i\}_1^n$, when the B-spline basis is given (including the knots points) and kept constant. A completely intrinsic affine invariant scale space is obtained via the affine geometric heat flow mentioned in the Introduction [36, 38].

Based on this affine invariance, we define now the B-spline affine invariant multiscale shape representation (*BAIM*) of the points $\{V_i\}_1^n$, as the family of curves C_k obtained from (3) for $k = 2, 3, \dots$

Figure 1⁴ presents the first *BAIM* example. The polygon contains 12 points. In Fig. 1(a), the initial

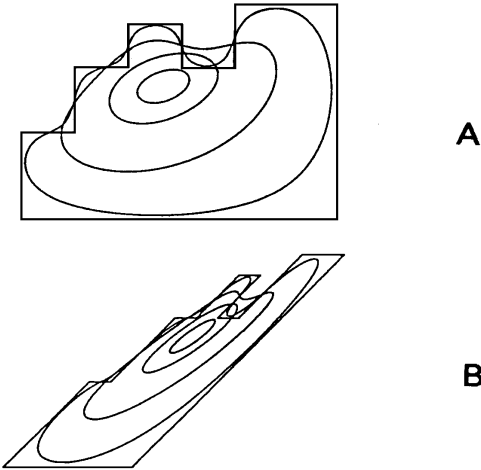


Figure 1. Example of the *BAIM* and its affine invariant property. A 12 points polygon (top) and its correspondent B-spline representations of order $k = 2^i$, $i = 1, 2, 4, 6, 7$. Note the convergence to the centroid, with an elliptical shape. In the bottom, the original polygon is obtained via an affine transformation of the one in the top. The corresponding *BAIM* is related by the same transformation.

polygon is given, together with the corresponding *BAIM* for $k = 2^i$, $i = 1, 2, 4, 6, 7$. In Fig. 1(b), the initial polygon is obtained via an affine transformation of the polygon in Fig. 1(a). Due to the affine invariant property, the corresponding *BAIM* is related to the one in Fig. 1(a) by the same affine transformation.

Note that when k increases ($k \rightarrow \infty$, see Fig. 1), the B-spline representation converges to the centroid of the initial polygon. The convergence is in such a way that the shape approaches an ellipse. This is obtained from the following theorem:

Theorem 1. *As k increases ($k \rightarrow \infty$), the B-spline representation converges to the centroid of the control points $\{V_i\}_1^n$, its shape becoming elliptical.*

Proof: Let's represent the control points as complex numbers, i.e., $V_i = [x_i + jy_i]$. Then, using the Fourier series expansion of the basis functions $B_{i,k}(u)$ [40, 41], we have that:

$$\begin{aligned} C_k(u) &= \sum_{i=1}^n V_i B_{i,k} \\ &= \sum_{i=1}^n (x_i + jy_i) \left[\sum_{m=-\infty}^{m=\infty} \exp\{jm\pi i\} \right. \\ &\quad \left. \times \left(\frac{2 \sin(m\pi/2)}{m\pi} \right)^k \exp\{jm\pi u\} \right] \\ &= \sum_{m=-\infty}^{m=\infty} \left(\sum_{i=1}^n (x_i + jy_i) \exp\{jm\pi i\} \right) \\ &\quad \times \left(\frac{2 \sin(m\pi/2)}{m\pi} \right)^k \exp\{jm\pi u\}. \end{aligned}$$

We see that when k increases ($k \rightarrow \infty$), the B-spline representation converges to the centroid of the initial polygon (only the term for $m = 0$ remains in the sum). Furthermore, the convergence is in such a way that the curve shape approaches an ellipse. This is so since high frequency components of the Fourier transform of the *BAIM* die out much faster than the low frequency ones. Therefore, the limiting curve becomes approximately an ellipse, when only the zero ($m = 0$) and first ($m = \pm 1$) frequency components remain significant. \square

As pointed out in the Introduction, a curve evolving according to the affine geometric heat flow, also converges to a point with elliptical shape [36–39]. In [7], the authors presented a discrete polygonal model of

the affine heat flow, and proved, also using Fourier decomposition, that the limiting polygon approaches an ellipse. These results are expected, since all of these three processes are affine smoothing process [7, 38, 41], and the ellipse is the most smooth affine invariant shape, being the only closed curve with constant affine curvature [35].

Before referring to a number of properties of this representation, let's remark basic differences between the *BAIM* and most scale-spaces as those presented at the Introduction:

1. Scale-spaces are usually motivated and defined over continuous curves and then discretized. The *BAIM* is directly derived from a set $\{V_i\}$ of discrete points. These set of points can be a dense sampling of the curve (even with $n \rightarrow \infty$), but it is always a discrete set. The smoothed curves, in contrast, are continuous, given as a linear combination of basis functions. This permits the easy computation of different curve properties (see also [17]).
2. The multiscale representation obtained via scale-spaces is usually continuous ($t \in [0, \tau)$), while the one obtained from the *BAIM* is discrete ($k = 2, 3, \dots$). See Section 4.

We discuss now, for the *BAIM*, the properties of scale-spaces presented in the Introduction. First note that for $k = 2$, the original set of points, or the polygon defined by them, is obtained. Therefore, the representation is complete.

The curve obtained from the B-spline representation (3) lies in the convex hull of at most k consecutive control points (those which affect the curve at the given point). For other relations between the control points, and the obtained B-spline, see [9]. Then, the order preserving property given in the Introduction, refers to the corresponding convex-hull for the *BAIM*, as well as to the other relations between control points and B-splines given in [9]. Note that when processing isolated shapes, this property is not so crucial in all applications. It becomes important for example when dealing with level sets of images as in [1].

The ‘‘causality’’ criteria holds, since for increasing k , increasingly smoother versions of the initial curve are obtained (see Figs. 1 and 2). Note that when k increases, both the basis functions get smoother, and the curve values are obtained as the weighted mean of more control points. The *BAIM* is a smoothing process with increasing smoothing exponent [41], in the sense that the total difference of any order decreases

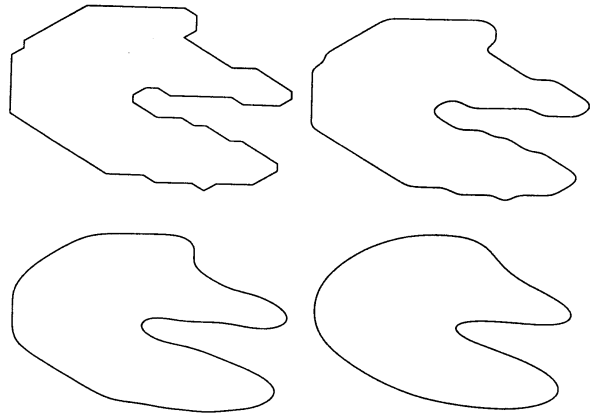


Figure 2. The smoothing property of the *BAIM* is shown in this example (orders 4, 20, and 90). The curve is getting more and more smooth when the order of the B-spline approximation is increased.

when k increases (*diminishing property*). The following geometric results can be proven as well, in relation with the smoothing property of B-spline representations. The first result, due to Lane and Riesenfeld [29], refers to the *geometric diminishing property*, and basically shows that the B-spline representation does not ‘‘oscillates’’ more than the given set of control points:

Theorem 2. *Every hyperplane of \mathbb{R}^m intersects a B-curve in \mathbb{R}^m no more often than the associated control polygon.*

One of the possible requirements related to the causality criteria is that the number of inflection points, zero crossings of the curvature, decreases when the scale increases. The following result, due to Goodman [19], states this.

Notation:

1. For $\mathcal{C}_0 = (x_0, y_0)$ and $\mathcal{C}_1 = (x_1, y_1)$, we define $\mathcal{C}_0 \times \mathcal{C}_1 := x_0y_1 - y_0x_1$.
2. $i(\mathcal{C})$ — number of inflections in the curve $\mathcal{C} \in \mathbb{R}^2$.
3. $S(\mathbf{a}) = S(\mathbf{a}_1, \dots, \mathbf{a}_n)$ — number of strict sign changes in the sequence $\mathbf{a} \in \mathbb{R}^2$.
4. $S(f)$ — number of strict changes in the function $f : (a, b) \rightarrow \mathbb{R}$. $S(f) = \sup S(f(t_1), \dots, f(t_n))$, where the supremum is taken over all the sequences $a < t_1 < \dots < t_n < b$.

The following definitions present a concept of curvature and curvature sign changes for \mathbb{C}^1 curves and polygons. This is necessary since the control points do

not form a \mathbb{C}^2 curve. Recall that the curvature κ of a \mathbb{C}^2 curve is defined as the rate of change of the tangent \mathcal{T} to the curve, and can be computed as $\kappa := \mathcal{C}_s \times \mathcal{C}_{ss}$ where s is the arc-length, and therefore \mathcal{C}_s is the tangent [42]. The definitions below are based on approximations of tangent vectors for non \mathbb{C}^2 curves.

Definition 1. Suppose $\mathcal{C} : [a, b] \rightarrow \mathbb{R}^2$ is continuous with piecewise \mathbb{C}^1 tangent vector

$$v := \frac{\mathcal{C}'}{|\mathcal{C}'|},$$

where $\mathcal{C}' = \frac{\partial \mathcal{C}}{\partial t}$. For $t \in (a, b)$, $\kappa(t)$ is defined such that it is positive (negative) if the curve is turning anti-clockwise (clockwise) at $\mathcal{C}(t)$. Suppose the curve is constant at $[\alpha, \beta] \subset (a, b)$, but not in any other larger interval. Then, we define

$$\kappa(t) := \begin{cases} \frac{1}{2}[v(\alpha^-) \times v'(\alpha^-) + v(\beta^+) \times v'(\beta^+)] & \text{if } v(\alpha^-) = v(\beta^+) \\ v(\alpha^-) \times v'(\beta^+) & \text{if } v(\alpha^-) \neq v(\beta^+) \end{cases}$$

Finally,

$$i(\mathcal{C}) := S(\kappa).$$

Definition 2. If the curve \mathcal{C} is a polygon, as the control polygon $\{V_i\}_1^n$, we write

$$I_i := (V_i - V_{i-1}) \times (V_{i+1} - V_i),$$

and

$$i(\{V_i\}_1^n) := S(I_1, \dots, I_N).$$

The following definition limits the class of control points for which the behavior of $i(\cdot)$ is analyzed. The idea is to limit the polygon such that it cannot turn too sharply.

Definition 3. The polygon $\{V_i\}_1^n$ is regular if the following hold:

1. It turns to a total angle of magnitude at most π , that is, for some vector $V \in \mathbb{R}^2$, $V \cdot (V_i - V_{i-1}) \geq 0$, $i = 0, 1, \dots, n$.
2. It does not turn through an angle of π at any vertex, i.e., $(V_i - V_{i-1}) \neq \lambda(V_i - V_{i+1})$ for any real λ .

Having all these definitions, we can now relate the behavior of the zero crossings of the B-spline \mathcal{C} with those of its control points:

Theorem 3. *If the control polygon $\{V_i\}_1^n$ is regular, then for the B-spline representation \mathcal{C} obtained from it via (3), the following relation holds:*

$$i(\mathcal{C}) \leq i(\{V_i\}_1^n).$$

Theorem 3 means that if the control polygon does not turn too sharply, then the number of inflection points of the B-spline representation does not exceed the number of inflections points at the control polygon. This result also holds for a large class of basis functions [16].

From the results above, we conclude that when moving from the control polygon to a B-spline representation, no ‘‘information’’ is added.

As pointed out in the Introduction, when scale-spaces are obtained as solutions of evolution equations, the causality criteria is usually connected to the semi-group property. We want to investigate now this property in a qualitative form. First note that the B-spline basis is obtained via repeated convolution of the Haar function, i.e.,

$$B_k = \chi * B_{k-1},$$

where χ is the indicator function. Therefore, the semi-group property holds for the basis of the representation.

Assume now that given the series of control points $\{V_i\}_1^n$, the corresponding B-spline representations \mathcal{C}_{k_1} and \mathcal{C}_{k_2} of order k_1 and k_2 respectively are computed ($k_1 < k_2$). Then, in relation to the semi-group property, we ask if we can compute (or at least approach) \mathcal{C}_{k_2} from \mathcal{C}_{k_1} . From (3) we have

$$\begin{aligned} \mathcal{C}_{k_1}(u) &= \sum_i^n V_i B_{i,k_1}, \\ \mathcal{C}_{k_2}(u) &= \sum_i^n V_i B_{i,k_2}. \end{aligned}$$

For computing a B-spline representation, we need a discrete set of control points. Therefore, \mathcal{C}_{k_1} is sampled:

$$\{\hat{V}_i\}_1^n := \{\mathcal{C}_{k_1}(u^i)\}_1^n = \left\{ \sum_j^n V_j B_{j,k_1}(u^i) \right\}_1^n,$$

and the sampling points are used for the computation

of a new B-spline approximation of order k_2 :

$$\begin{aligned}\hat{\mathcal{C}}_{k_2}(u) &= \sum_i^n \hat{V}_i B_{i,k_2} \\ &= \sum_i^n \left(\sum_j^n V_j B_{j,k_1}(u^i) \right) B_{i,k_2}.\end{aligned}$$

The difference between \mathcal{C}_{k_2} and $\hat{\mathcal{C}}_{k_2}$ is given by:

$$\begin{aligned}\|\mathcal{C}_{k_2} - \hat{\mathcal{C}}_{k_2}\| &= \left\| \sum_i^n V_i B_{i,k_2} - \sum_i^n \left(\sum_j^n V_j B_{j,k_1}(u^i) \right) B_{i,k_2} \right\| \\ &= \left\| \sum_i^n \left[V_i - \sum_j^n V_j B_{j,k_1}(u^i) \right] B_{i,k_2} \right\| \\ &\leq \sum_i^n \left\| V_i - \sum_j^n V_j B_{j,k_1}(u^i) \right\| B_{i,k_2} \\ &\leq \Upsilon(k_1, \{V_i\}) \sum_i^n B_{i,k_2} \\ &= \Upsilon(k_1, \{V_i\}),\end{aligned}$$

where $\Upsilon(k, \{V_i\})$ is a bound on the distance between the control points and the B-spline of order k . General bounds for the distance between the initial polygon and the corresponding B-spline representation can be found in [9]. Note that since the B-spline basis are normalized, we have

$$\begin{aligned}\left\| V_i - \left(\sum_j^n V_j B_{j,k_1}(u^i) \right) \right\| B_{i,k_2} \\ = \left\| \sum_j^n (V_i - V_j) B_{j,k_1}(u^i) \right\| B_{i,k_2},\end{aligned}$$

and the error is like a weighted average of the difference between the control points (only those which affects the value at u^i).

Since the bound Υ increases with k [9], so does the error bound. On the other hand, the shape of the spline approximations is similar to the original curve, then it is expected from the shapes \mathcal{C}_{k_2} and $\hat{\mathcal{C}}_{k_2}$ to be similar as well. The error can also be reduced if $\hat{\mathcal{C}}_{k_1}$ is sampled in such a way that the points $\hat{\mathcal{C}}_{k_1}(u^i)$ are as close as possible to V_i . This property was experimented and the results are shown in Fig. 3. The original polygon is given in Fig. 3(a). The B-spline representations of order 5, 10, and 15 were computed (Figs. 3(b)–(e)). Then, the B-spline of order $k_1 = 5$ (Fig. 3(b)) is uniformly

sampled, and represented by the same number of points as the original polygon. After that, the B-splines of order (k_2) 10 and 15 were computed, with this polygon as initial data (Figs. 3(f) and 3(g)). As expected, the obtained B-spline representations are very similar to the ones obtained with the original polygon in Fig. 3(a). (When Figs. 3(b), 3(f), and Figs. 3(c), 3(g), are presented in the same draw, almost no distinction between the corresponding curves is obtained.) Small difference were observed when k_1 is increased, but the general (qualitative) shape was always preserved. Therefore, we can conclude that the semi-group property holds in a qualitative form.

3.1. The BAIM of Continuous Initial Curves and Noisy Polygons

If the original curve is given in a continuous form (by a formula for example), then the curve must be sampled in order to construct the *BAIM*. This is in fact what we did in Fig. 3 for the construction of Figs. 3(f) and 3(g).

Since we are interested in an affine invariant representation, the ideal situation is to do the sampling in an affine invariant form. This can be done for example starting from the point of maximal *affine curvature*, and sampling the curve at constant *affine distance*. These properties are conserved under an affine transformation [6]. In this way, the sampling points (control vertices) are affine invariant. Note also that since the *BAIM* is given as a linear combination of B-spline basis functions, geometric properties of the curve, as affine curvature, can be computed directly, using the classical formulas for derivatives [9]. For instance, it is well known that derivatives of B-splines can be obtained taking finite differences of lower order splines.

If the sampling strategy described above cannot be performed (due to the presence of noise for example), then, a regular sampling can be performed. Since the B-spline basis is normalized, the error of the *BAIM* is controlled by the error in the control vertices coordinates. In other words, if the error in the control vertices coordinates is bounded by ϵ , so is the error in the B-spline representation coordinates. Figures 4 and 5 show examples of the *BAIM* of noisy initial curves. Note that when k increases, the noise in a given control point extends to bigger segments in the curve (the support of $B_{i,k}$ gets bigger). On the other hand, increasing k , also increases the number of control points which participates in the weighted mean (3) for each point $\hat{\mathcal{C}}_k(u)$, decreasing the influence of the error in a given control point.

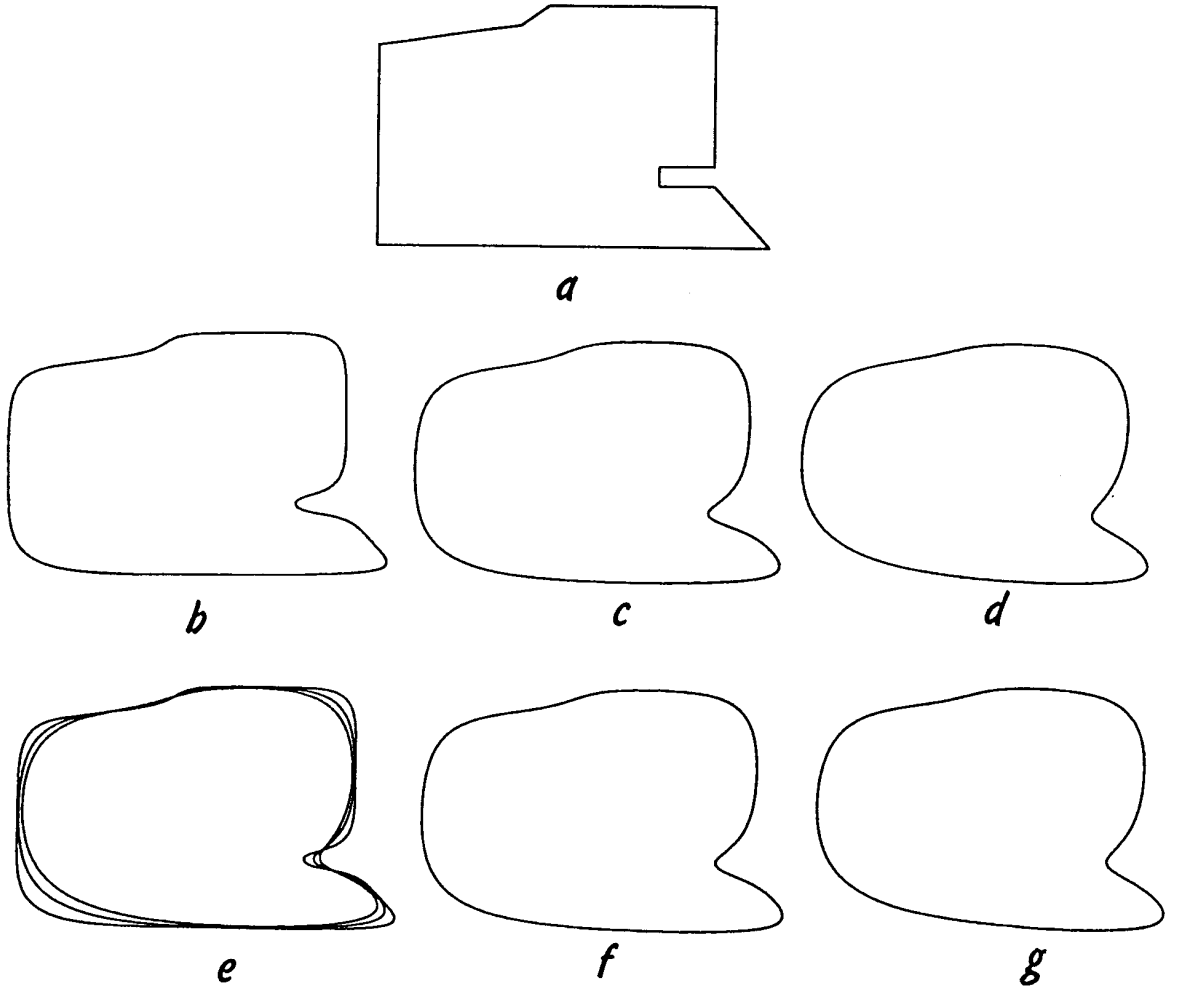


Figure 3. Investigation of the semi-group property for the BAIM: (a) The original polygon, (b) B-spline representation of order 5, (c) B-spline representation of order 10, (d) B-spline representation of order 15, (e) B-spline representations of orders 5, 10, and 15, (f) B-spline representation of order 10 obtained from the sampling of the curve in (b), (g) B-spline representation of order 15 obtained from the sampling of the curve in (b).

4. Continuous-Scale B-Splines

The multiscale representation described so far is discrete in the sense that the B-splines $B_{0,k} = (*)^k \chi_{[0,1]}$ that are used to generate it are indexed by a discrete parameter $k \in \mathbb{N} - \{0\}$. In order to obtain a continuous multiscale representation, one needs to extend these generators to a family of compactly supported functions $B_{0,r}$, $r \in [0, +\infty)$, that coincides with the previous one on the integer values of r .

The semi-group property of the multiscale representation is expressed in the integer case by the relation

$B_{0,k} = B_{0,k-1} * \chi_{[0,1]}$ indicating that $B_{0,k}$ is obtained by smoothing $B_{0,k-1}$. To preserve this causality, we would like that for $r_1 > r_2$, B_{0,r_1} is obtained by as smoothing operation applied to B_{0,r_2} . Recall that if f is in \mathbf{C}^n but not in \mathbf{C}^{n+1} , then its (global) Hölder exponent is given by $\mu(f) = n + \nu$ with

$$\nu = \inf_x \left(\liminf_{|t| \rightarrow 0} \frac{\log |f^{(n)}(x+t) - f^{(n)}(x)|}{\log |t|} \right), \quad (8)$$

where $f^{(n)}$ is the n -th derivative of the function f . If

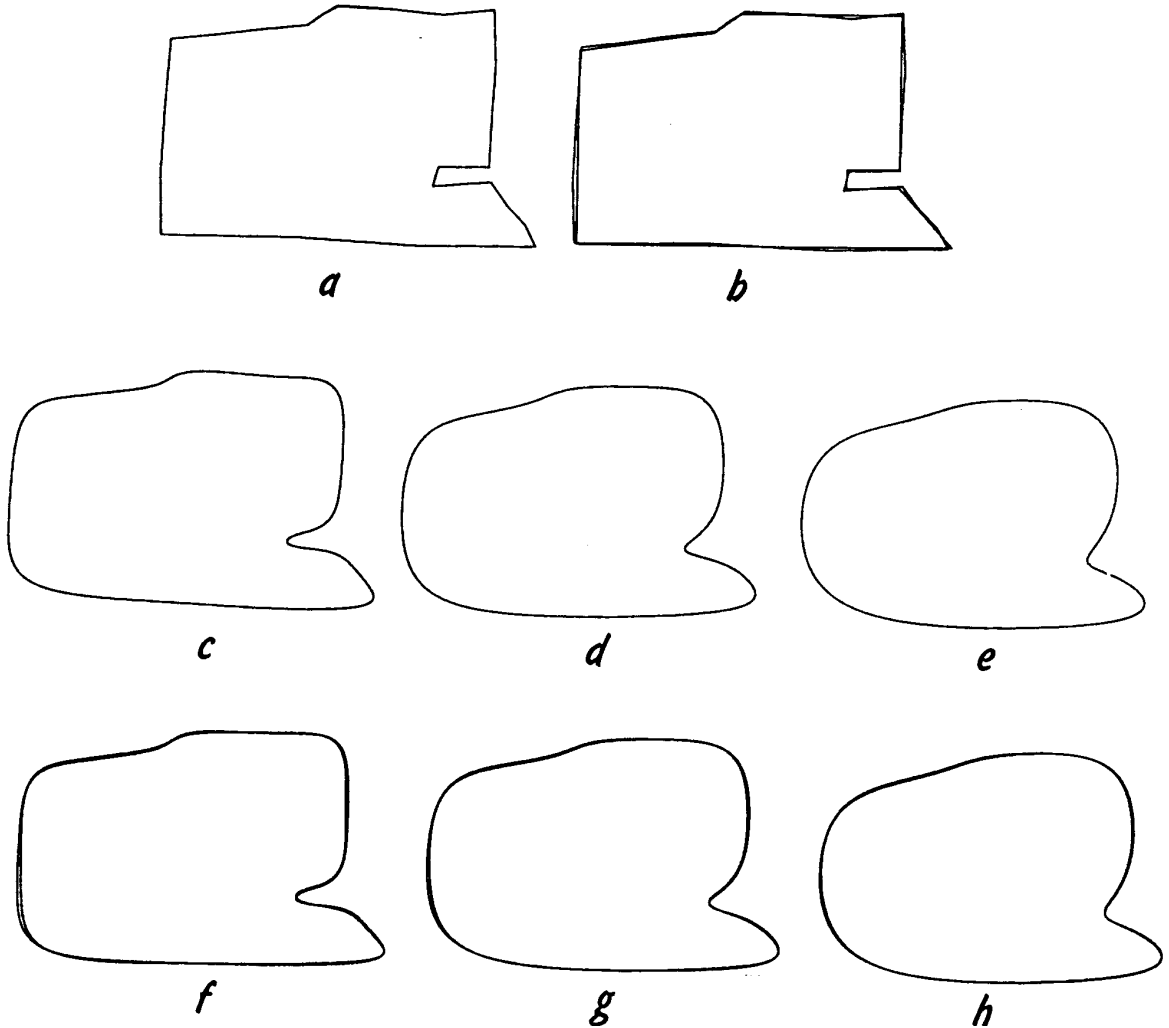


Figure 4. The BAIM of a noisy curve: (a) the original polygon. The polygon was obtained from the one in Fig. 3(a) adding random noise to the coordinates, (b) original and noisy polygons, (c) B-spline representation of order 5, (d) B-spline representation of order 10, (e) B-spline representation of order 15, (f) B-spline representation of order 5 of the original and noisy polygons, (g) B-spline representation of order 10 of the original and noisy polygons, (h) B-spline representation of order 15 of the original and noisy polygons.

we use of Hölder exponent to measure the regularity c our generators, we would like to have

$$r_1 > r_2 \Rightarrow \mu(B_{0,r_1}) > \mu(B_{0,r_2}). \quad (9)$$

A straightforward technique to extend the B-spline family is to define for $r = k+s, k \in \mathbb{N} - \{0\}, s \in [0, 1]$,

$$B_{0,r} = (1-s)B_{0,k} + sB_{0,k+1}. \quad (10)$$

With such a definition, it is clear however that the

property (9) will not be satisfied since we have, for all $0 \leq s < 1, \mu(B_{0,k+s}) = \mu(B_{0,k}) = k - 1$.

We shall thus use a more sophisticated extension of the B-spline family. This extension is based on “subdivision schemes” that are frequently used in computer-aided geometric design [15, 28].

Subdivision schemes constitute a useful tool for the fast generation of smooth curves and surfaces from a set of control points by means of iterative refinements. In the most often considered binary unidimensional case, one starts from a sequence $s_0(i)$ and obtains at step j

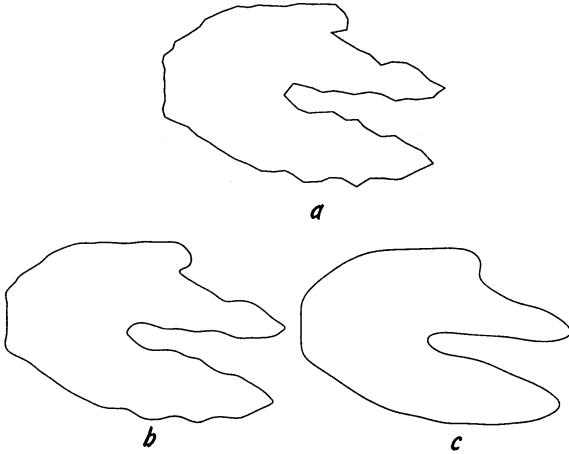


Figure 5. A second example of the BAIM of a noisy curve (compare with Fig. 2): (a) The noisy curve, (b) B-spline representation of order 4, (c) B-spline representation of order 20.

a sequence $s_j(2^{-j}i)$, generated from the previous one by linear rules:

$$\begin{aligned} s_j(2^{-j}2i) &= \sum_n a_{j,i}(n)s_{j-1}(2^{-j+1}(i-n)), \\ s_j(2^{-j}(2i+1)) &= \sum_n b_{j,i}(n)s_{j-1}(2^{-j+1}(i-n)). \end{aligned} \quad (11)$$

The masks $a_{j,i}(n)$ and $b_{j,i}(n)$ are in general finite sequences, a property that is clearly useful for the practical implementation of (11).

Equation (11) means that the new series of points s_{j+1} is obtained as a linear combination of the series s_j , starting from the control points s_0 . Different selections of the mask will give different series s_j . A natural problem is then to study the convergence of such an algorithm to a limit function when $j \rightarrow \infty$. In particular, the scheme is said to be strongly convergent if and only if there exists a continuous function $f(x)$ such that $\lim_{j \rightarrow +\infty} (\sup_i |s_j(2^{-j}i) - f(2^{-j}i)|) = 0$. One can study more general type of convergence with the use of a smooth function g that is well localized in space (for example compactly supported) and satisfies the interpolation property $g(i) = \delta_i$. One can then define $f_j(x) = \sum_i s_j(2^{-j}i)g(2^jx - i)$ and study the convergence in a functional sense of f_j to f .

A subdivision scheme is said to be stationary when the masks a and b are independent of the parameters j and i . In that case, the limit $f(x)$ is given by

$$f(x) = \sum_{i \in \mathbb{Z}} s_0(i)\varphi(x-i), \quad (12)$$

where φ is the limit function obtained from the Dirac sequence $s_0(i) = \delta_{0,i}$. For this reason φ is often called the “limit function” of the stationary subdivision. Therefore, for a given set of stationary mask a and b , having the control points s_0 is enough to determine the final curve f , having computed a priori the limit function φ . One can also rewrite (11) as

$$s_j(2^{-j}i) = \sum_n c(i-2n)s_{j-1}(2^{-j+1}n), \quad (13)$$

with $c(2i) = a(i)$ and $c(2i+1) = b(i)$. Note that (11) is equivalent to fill the sequence s_{j-1} with zeros at the intermediate points $2^{-j}(2i+1)$ and apply a discrete convolution with the sequence $c(i)$. As a consequence, the function φ is the result of an infinite number of discrete convolutions at finer and finer scales. It can also be expressed in the Fourier domain by the infinite product

$$\hat{\varphi}(\omega) = \prod_{j=1}^{+\infty} m(2^{-j}\omega), \quad (14)$$

where $m(\omega) = \frac{1}{2} \sum_n c(n)e^{-in\omega}$ is a 2π -periodic function. Note that if $c(n) = 0$ for $n < a$ and $N > b$, i.e., $m(\omega)$ is a finite Fourier series, then φ is compactly supported in $[a, b]$.

Equation (14) means that the design of a subdivision scheme can be performed in the Fourier domain, via the design of the Fourier transform m of the mask c . This will be crucial in order to obtain continuous scale B-splines below.

Detailed reviews of stationary subdivision and their possible generalizations have been done by Cavaretta, Dahmen and Micchelli in [11] and Dyn in [15].

The B-spline $B_{0,k}$ can be viewed as the limit function of a stationary subdivision scheme associated to the trigonometric polynomial⁵

$$m_k(\omega) = \left(\frac{1 + e^{-i\omega}}{2} \right)^k, \quad (15)$$

since we have indeed

$$\hat{B}_{0,k}(\omega) = \left(\frac{1 + e^{-i\omega}}{\omega} \right)^k = \prod_{j=1}^{+\infty} m_k(2^{-j}\omega). \quad (16)$$

Note that the coefficients of the subdivision are given by $c_k(n) = 2^{-k+1} \binom{k}{n}$ for $n = 0 \dots k$. It is thus possible to use the above described subdivision algorithm to generate the B-spline discrete representation in a very fast way.

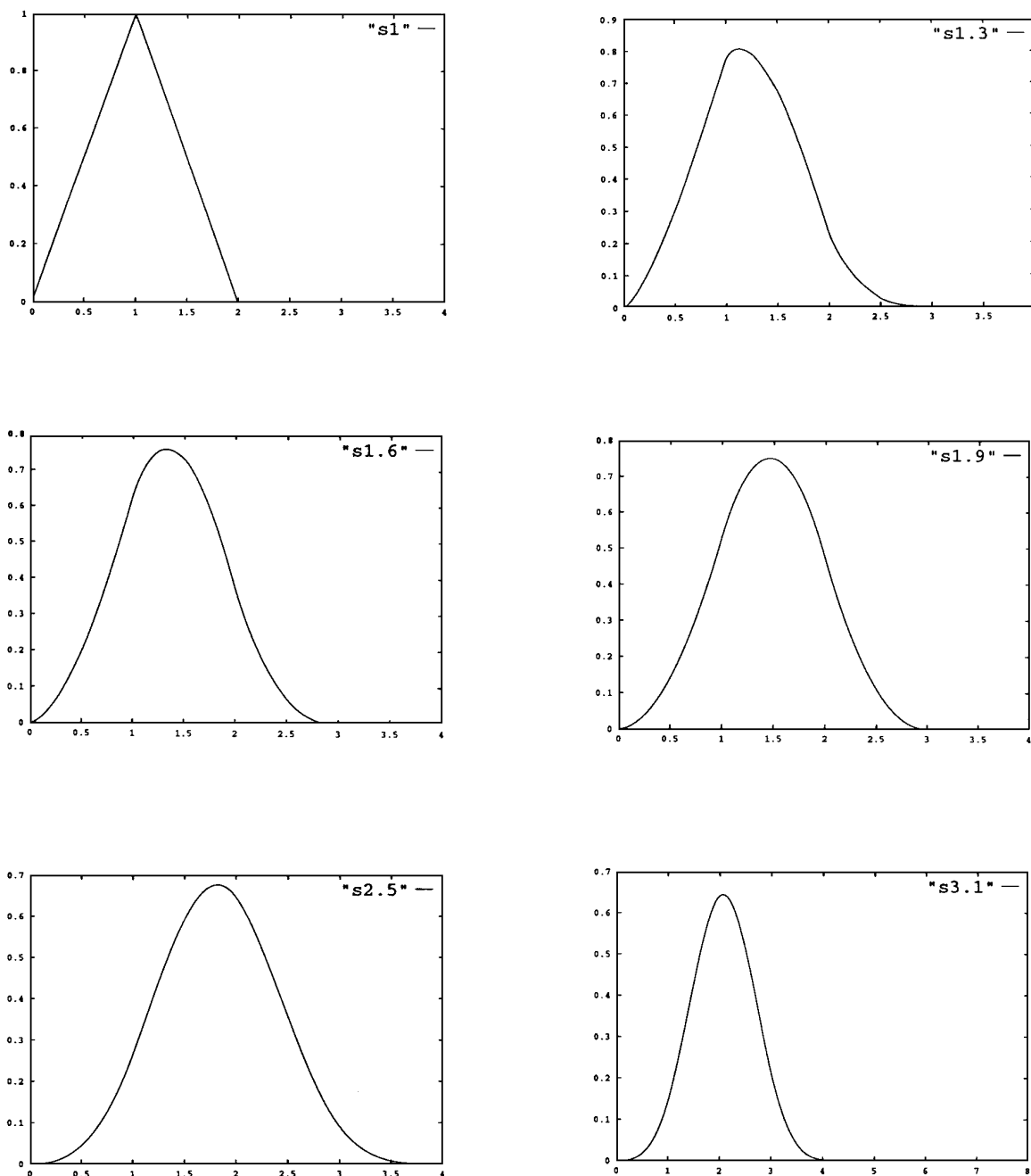


Figure 6. Example of continuous scale B-spline basis functions $B_{0,r}(u)$, $r \in \mathbb{R}^+$. The splines orders r are given in the graphs.

(Continued on next page)

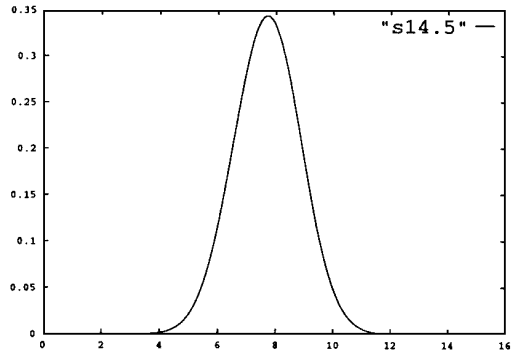
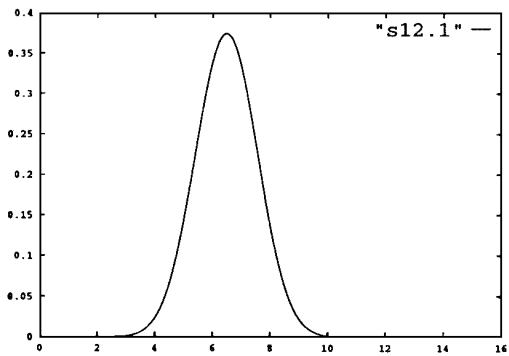
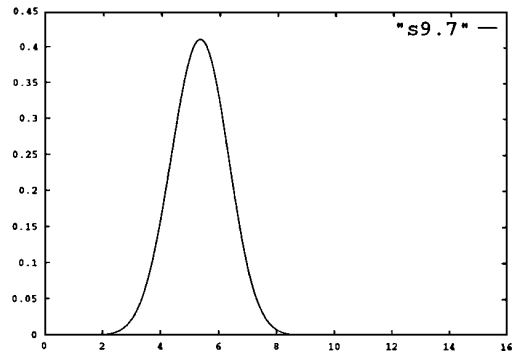
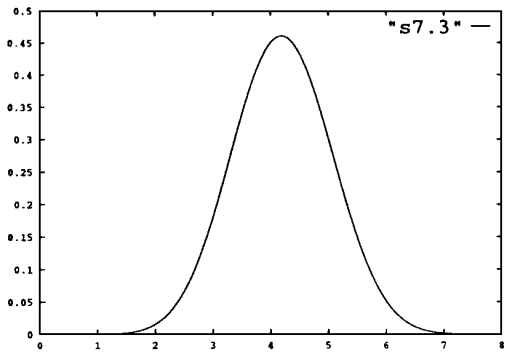
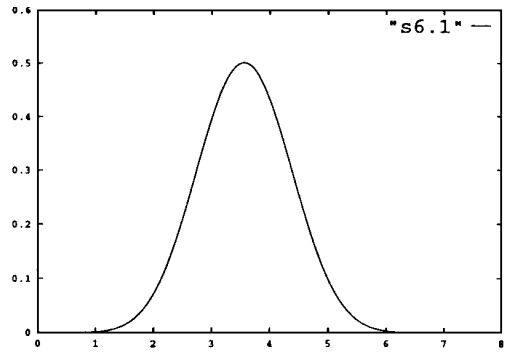
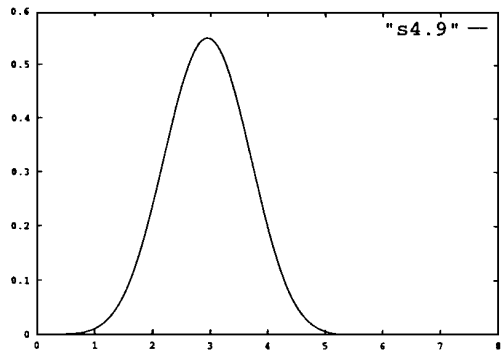


Figure 6. (Continues.)

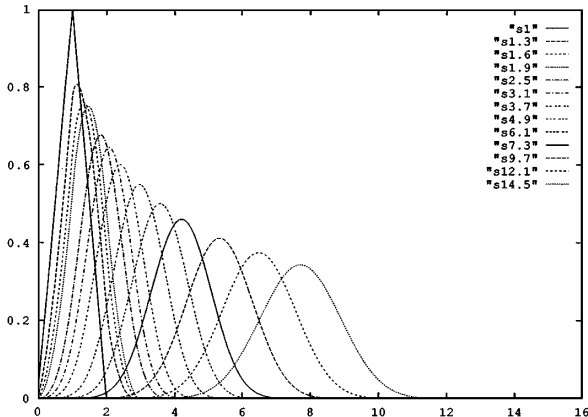


Figure 6. (Continued.)

In order to extend the B-splines to continuous scale, we have to compute a new function m_r , $r \in \mathbb{R}^+$, which will define via (14) the Fourier transform $\hat{\varphi}$ of the limit function φ , that is, the continuous scale B-spline. Having computed φ , the continuous scale representation is obtained via (12), as in the classical case of discrete scale B-spline representations. We shall now generate this continuous parameter representation by interpolating between the functions $m_k(\omega)$. We shall thus define for $r = k + s$, $k \in \mathbb{N} - \{0\}$, $s \in [0, 1]$,

$$\begin{aligned} m_r(\omega) &:= \left(\frac{1 + s e^{-i\omega}}{1 + s} \right) \left(\frac{1 + e^{-i\omega}}{2} \right)^k \\ &= \frac{1}{2} \sum_n c_r(n) e^{-in\omega}. \end{aligned} \quad (17)$$

Note that m_r above is obtained from the function m_k corresponding to classical B-splines by multiplication with $\frac{1 + s e^{-i\omega}}{1 + s}$. Other functions m_r can be computed, as for example replacing the discrete exponent k in (15) by the continuous one r . This will give a limit function φ with non-compact support, making the extended continuous scale B-splines non-local and not useful for real computations.

From m_r we obtain that our continuously parametrized B-spline $B_{0,r}$ will then be defined by (the Fourier transform)

$$\hat{B}_{0,r}(\omega) := \prod_{j=1}^{+\infty} m_r(2^{-j}\omega). \quad (18)$$

These functions are compactly supported in $[0, k + 1]$ for $k < r \leq k + 1$. Their regularity can be studied by several techniques. Many contributions have been made to the problem of estimating the regularity of the

limit functions of subdivision schemes, due to the diverse possible definitions of regularity. For the Hölder exponent, a method that leads to an exact estimate is described in Daubechies and Lagarias [12]. Applied to our particular limit functions, this method can be summarized as follows: One defines two infinite matrices $(T_\varepsilon)_{i,j} = c_s(2i - j - \varepsilon + 1)$, $\varepsilon = 0, 1$ and study their action on the stable subspace E of the sequences $\{\dots, 0, 0, s_1, s_2, 0, 0, \dots\}$. The Hölder exponent of $B_{0,r} = B_{0,k+s}$ is then given by

$$\mu(B_{0,r}) = k - \log_2 \rho(T_0, T_1), \quad (19)$$

where $\rho(T^0, T^1)$ is the “joint spectral radius” of T_0 and T_1 , defined by

$$\begin{aligned} \rho(T^0, T^1) &:= \limsup_{m \rightarrow +\infty} \left(\max_{\varepsilon_j=0 \text{ or } 1} \|T_{\varepsilon_1} T_{\varepsilon_2} \cdots T_{\varepsilon_m}\|_E^{1/m} \right). \end{aligned} \quad (20)$$

In E , the operators T_0 and T_1 are given by the two matrices

$$M_0 = \frac{2}{1+s} \begin{pmatrix} 1 & 0 \\ 0 & s \end{pmatrix} \quad \text{and} \quad M_1 = \frac{2}{1+s} \begin{pmatrix} s & 1 \\ 0 & 1 \end{pmatrix}. \quad (21)$$

One checks easily that we have in that case $\rho(T_0, T_1) = \|T_0\| = \frac{2}{1+s}$ and we thus have that the Hölder exponent for our continuous scale B-splines is given by

$$\mu(B_{0,r}) = k - 1 + \log_2(1 + s). \quad (22)$$

This formula shows in particular that the smoothing property (9) is satisfied by this construction of m_r . Note also, from Eq. (17) that the defined continuously parametrized B-spline basis coincides with the classical one for integer scales, i.e., for $s = 0, 1$. Other important properties of classical B-splines, as the normalization (see Section 2) can be showed for the extended basis as well.

Figure 6 shows the graphs of $B_{0,r}(u)$ for different values of r . The splines orders are given in the graphs. For $k \leq r \leq k + 1$, all basis supports are in the same interval, corresponding to the interval between the supports of $B_{0,k}$ and $B_{0,k+1}$. An example of a continuously parametrized B-spline representation is given in Fig. 7 (the original control shape is in the top left corner). Note how the shape becomes more and more smooth when r increases, even for r values in the same interval $[k, k + 1]$.

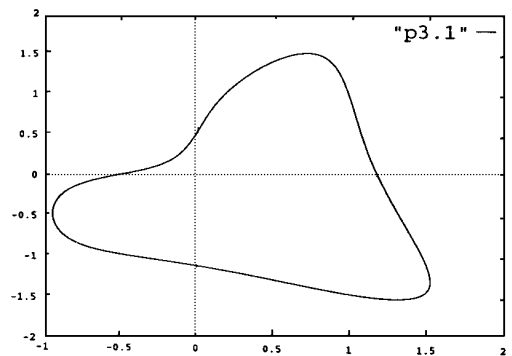
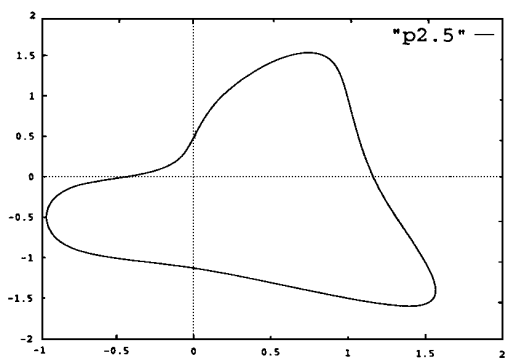
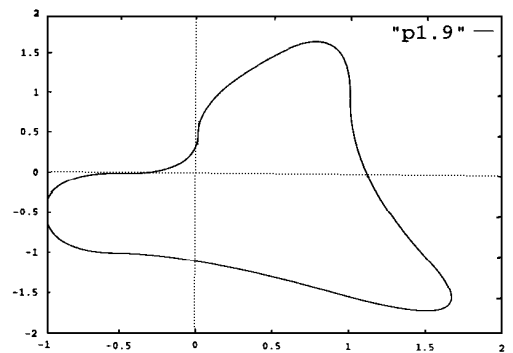
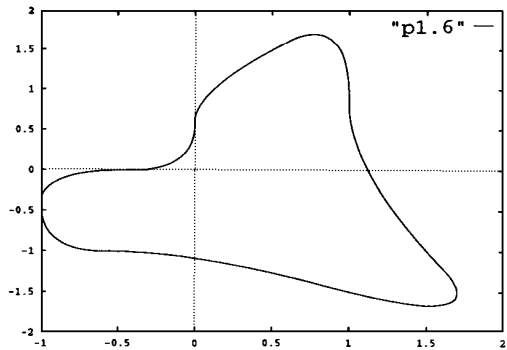
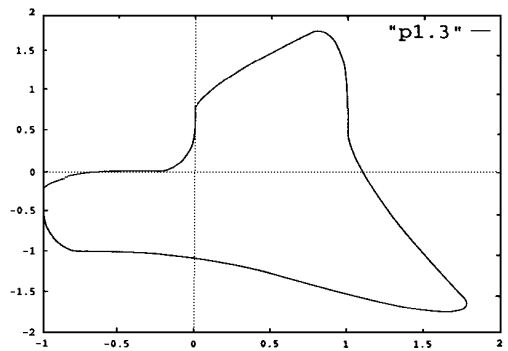
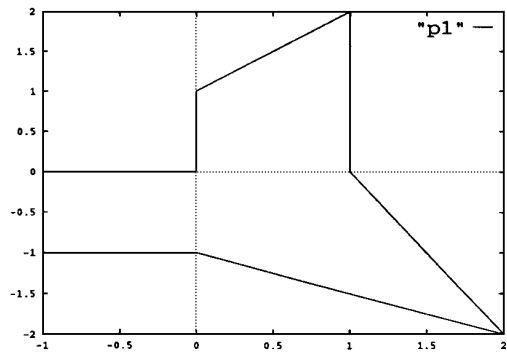


Figure 7. Example of continuous scale B-spline representation. The splines orders r are given in the graphs. The original control points are given in the top left corner. *(Continued on next page)*

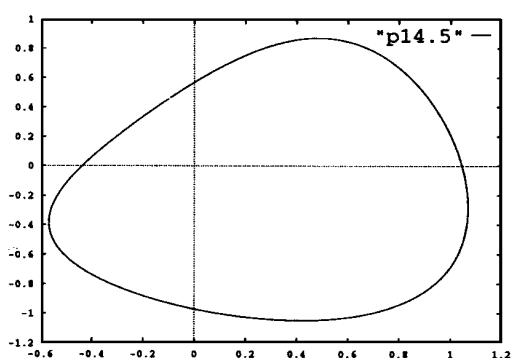
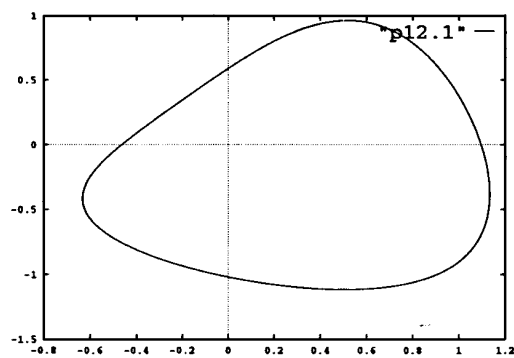
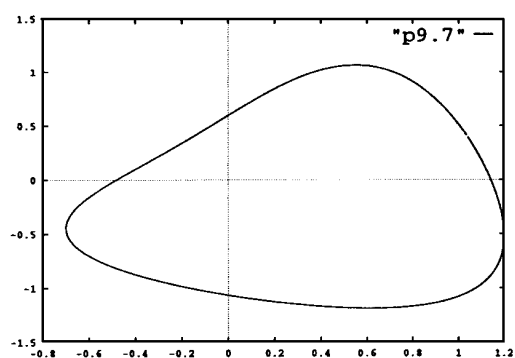
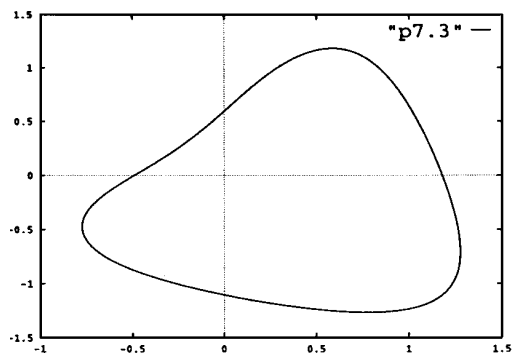
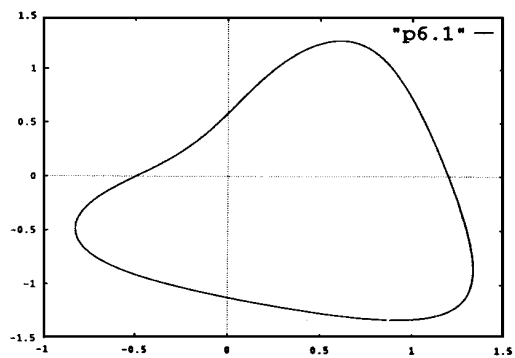
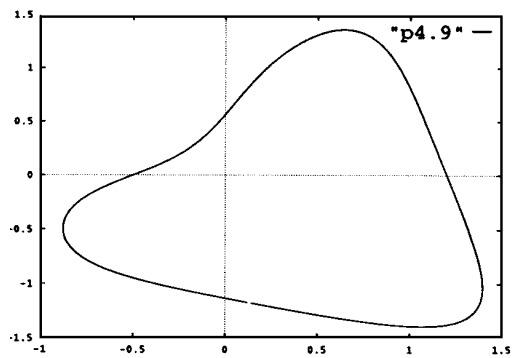


Figure 7. (Continues.)

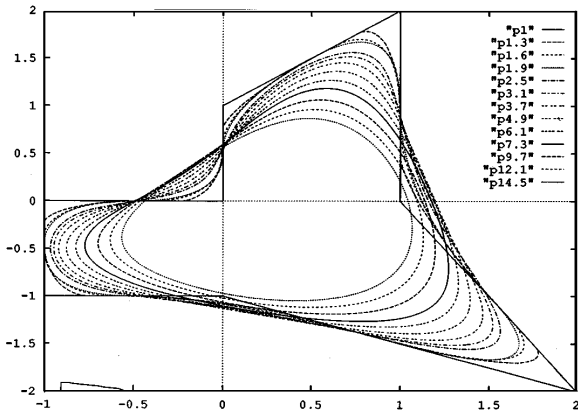


Figure 7. (Continued.)

5. Concluding Remarks

In this paper, an affine invariant multiscale shape representation was described. The representation is obtained via the computation of B-splines of increasing order, and therefore is affine invariant. The representation was first presented using classical B-splines, which are functions in C^{k-2} , obtaining a scale-space which is discrete in scale. We then extended, based on subdivision schemes, this basis to a continuous-scale one, that is, finite support functions in C^{k-2+r} , where $r \in [0, 1]$. When $r = 0$ or $r = 1$, the basis coincides with the classical B-spline one described here. Using this basis, the affine multiscale representation is extended to a continuous scale one as well.

We showed that the basic properties of continuous scale-spaces hold for this representation, at least in a qualitative form. We presented as well a number of geometric properties related to the smoothing behavior of B-spline representations. The proposed B-spline based multiscale representation is easily implemented using the recursive formula for the B-spline basis computation. In contrast with scale-spaces as the Gaussian one, it is defined directly on an initial discrete set of points, avoiding problems caused by discretization of continuous scale-spaces. The smoothed signal is continuous (and analytical), allowing straightforward computation of geometric properties of the smoothed curve, as curvature (this is a main difference with other discrete scale-spaces as the proposed in [30]). Therefore, the proposed representation is natural for computer shape analysis, since receives as input a digital signal, while keeping a continuous representation which can be helpful for different computations.

The same ideas presented in this paper hold for other basis based representation, as well as other subdivision schemes, which keep the basic properties described in this work. We described the basic approach using the classical B-spline, and its extension given in Section 4, because of its attractive properties, as those given in Section 2, and the existence of extensive analysis, which permits to conclude important geometric properties as the theorems presented in this paper.

Notes

1. In the case of the 1D Gaussian scale-space for example, zero crossings are not added.
2. Since the order k plays the (qualitative) role of scale, from now on we refer to k as the scale of the representation.
3. To deal with closed curves, the series of points are periodic, that is, the indices are computed modulo $n + 1$.
4. The examples here presented were implemented using the Matlab Spline Toolbox [10].
5. Recall that $B_{0,k}$ is obtained from the convolution of the indicator function.

References

1. L. Alvarez, F. Guichard, P.L. Lions, and J.M. Morel, "Axiomes et equations fondamentales du traitement d'images," *C.R. Acad. Sci.*, Paris, Vol. 315, pp. 135–138, 1992.
2. L. Alvarez, F. Guichard, P.L. Lions, and J.M. Morel, "Axiomatization et nouveaux operateurs de la morphologie mathematique," *C.R. Acad. Sci.*, Paris, Vol. 315, pp. 265–268, 1992.
3. L. Alvarez, P.L. Lions, and J.M. Morel, "Image selective smoothing and edge detection by nonlinear diffusion," *SIAM J. Numer. Anal.*, Vol. 29, pp. 845–866, 1992.
4. J. Babaud, A.P. Witkin, M. Baudin, and R.O. Duda, "Uniqueness of the Gaussian kernel for scale-space filtering," *IEEE Trans. Pattern Anal. Machine Intell.*, Vol. 8, pp. 26–33, 1986.
5. R.H. Bartles, J.C. Beatty, and B.A. Barsky, *An Introduction to Splines for Use in Computer Graphics and Geometric Modeling*, Morhan Kaufmann Publishers, Inc.: California, 1987.
6. W. Blaschke *Vorlesungen über Differentialgeometrie II*, Verlag Von Julius Springer: Berlin, 1923.
7. A.M. Bruckstein, G. Sapiro, and D. Shaked, "Evolutions of planar polygons," to appear, *International J. of Pattern Recognition and Artificial Intelligence*, Vol. 9, No. 6, pp. 991–1014, 1995.
8. M.H. Chen and P.F. Yan, "A multiscale approach based on morphological filtering," *IEEE Trans. Pattern Anal. Machine Intell.*, Vol. 11, pp. 694–700, 1989.
9. C. de Boor, "A practical guide to splines," *Applied Mathematical Sciences*, Vol. 27, Spinger-Verlag: New York, 1978.
10. C. de Boor, *Spline Toolbox for Use with MATLABTH*, The Math Works, Inc., Natick, 1990.
11. Cavaretta Dahmen and C.A. Micchelli, "Stationary subdivision," *Mem. Amer. Math. Soc.*, Vol. 93, pp. 1–186, 1991.
12. I. Daubechies and Lagarias, "Two-scale difference equations I: Existence and global regularity of solutions," *SIAM J. Math. Anal.*, Vol. 22, pp. 1388–1410, 1991.

13. J. Dieudonné and J. Carrell, *Invariant Theory: Old and New*, Academic Press: London, 1970.
14. G. Dudek and J.K. Tsotsos, "Shape representation and recognition from curvature," *Proceedings of the IEEE Conference on CVPR*, Hawaii, 1991.
15. N. Dyn, "Subdivision schemes in computer-aided geometric design," in *Wavelets, Subdivision Algorithms and Radial Basis Functions*, W. Light (Ed.), Oxford University Press: Oxford, 1992.
16. N. Dyn and C.A. Micchelli, "Piecewise polynomial spaces and geometric continuity of curves," *Numer. Math.*, Vol. 54, pp. 319–337, 1988.
17. L.M.J. Florack, B.M. ter Haar Romeny, J.J. Koenderink, and M.A. Viergever, "Scale and the differential structure of images," *Image and Vision Computing*, Vol. 10, pp. 376–388, 1992.
18. M. Gage and R.S. Hamilton, "The heat equation shrinking convex plane curves," *J. Differential Geometry*, Vol. 23, pp. 69–96, 1986.
19. T.N.T. Goodman, "Inflections on curves in two and three dimensions," *Computer Aided Geometric Design*, Vol. 8, pp. 37–50, 1991.
20. M. Grayson, "The heat equation shrinks embedded plane curves to round points," *J. Differential Geometry*, Vol. 26, pp. 285–314, 1987.
21. A. Hummel, "Representations based on zero-crossings in scale-space," *Proc. IEEE Computer Vision and Pattern Recognition Conf.*, pp. 204–209, 1986.
22. P. Kempenaers, L. Van Gool, and A. Oosterlink, "Shape recognition under affine distortions," in *Visual Form*, C. Arcelli et al. (Eds.), Plenum Press: New York, 1991.
23. B.B. Kimia, A. Tannenbaum, and S.W. Zucker, "Toward a computational theory of shape: An overview," *Lecture Notes in Computer Science*, Vol. 427, pp. 402–407, Springer-Verlag: New York, 1990.
24. B.B. Kimia, A. Tannenbaum, and S.W. Zucker, "Shapes, shocks, and deformations, I," to appear in *International Journals of Computer Vision*, Vol. 15, pp. 189–224, 1995.
25. J.J. Koenderink, "The structure of images," *Biological Cybernetics*, Vol. 50, pp. 363–370, 1984.
26. J.J. Koenderink, *Solid Shape*, MIT Press: Cambridge, MA, 1990.
27. J.J. Koenderink and A.J. van Doorn, "Representation of local geometry in the visual system," *Biological Cybernetics*, Vol. 55, pp. 367–375, 1987.
28. J.M. Lane and R.F. Riesenfeld, "A theoretical development for the computer generation and display of piecewise polynomial surfaces," *IEEE Trans. PAMI*, Vol. 2, pp. 35–46, 1980.
29. J.M. Lane and R.F. Riesenfeld, "A geometric proof for the variation diminishing property of B-spline approximation," *J. Approx. Theory*, Vol. 37, pp. 1–4, 1983.
30. T. Lindeberg, "Scale-space for discrete signals," *IEEE Trans. Pattern Anal. Machine Intell.*, Vol. 12, pp. 234–254, 1990.
31. F. Mokhtarian and A. Mackworth, "Scale-based description of planar curves and two-dimensional shapes," *IEEE Trans. Pattern Anal. Machine Intell.*, Vol. 8, pp. 34–43, 1986.
32. F. Mokhtarian and A. Mackworth, "A theory of multiscale, curvature-based shape representation for planar curves," *IEEE Trans. Pattern. Anal. Machine Intell.*, Vol. 14, pp. 789–805, 1992.
33. S.J. Osher and J.A. Sethian, "Fronts propagation with curvature dependent speed: Algorithms based on Hamilton-Jacobi formulations," *Journal of Computational Physics*, Vol. 79, pp. 12–49, 1988.
34. P. Perona and J. Malik, "Scale-space and edge detection using anisotropic diffusion," *IEEE Trans. Pattern. Anal. Machine Intell.*, Vol. 12, pp. 629–639, 1990.
35. G. Sapiro and A.M. Bruckstein, "The ubiquitous ellipse," *Acta Applicandae Mathematicae*, Vol. 38, pp. 149–161, 1995.
36. G. Sapiro and A. Tannenbaum, "On affine plane curve evolution," *Journal of Functional Analysis*, Vol. 119, No. 1, pp. 79–120, 1994.
37. G. Sapiro and A. Tannenbaum, "Affine shortening of non-convex plane curves," *EE Publication*, Vol. 845, Department of Electrical Engineering, Technion, I.I.T., Haifa 32000, Israel, July 1992.
38. G. Sapiro and A. Tannenbaum, "Affine invariant scale-space," *International Journal of Computer Vision*, Vol. 11, No. 1, pp. 25–44, 1993.
39. G. Sapiro and A. Tannenbaum, "On invariant curve evolution and image analysis," *Indiana Journal of Mathematics*, Vol. 42, No. 3, 1993.
40. I.J. Schoenberg, *Cardinal Spline Interpolation*, SIAM Press: Philadelphia, 1973.
41. I.J. Schoenberg, *Selected Papers II*, C. de Boor (Ed.), Birkhauser: Boston, 1988.
42. M. Spivak, *A Comprehensive Introduction to Differential Geometry*, Publish or Perish Inc.: Berkeley, California, 1979.
43. A.P. Witkin, "Scale-space filtering," *Int. Joint. Conf. Artificial Intelligence*, pp. 1019–1021, 1983.
44. A.L. Yuille and T.A. Poggio, "Scaling theorems for zero crossings," *IEEE Trans. Pattern Anal. Machine Intell.*, Vol. 8, pp. 15–25, 1986.



Guillermo Sapiro was born in Montevideo, Uruguay, on April 3, 1966. He received his B.Sc. (summa cum laude), M.Sc., and Ph.D. from the Department of Electrical Engineering at the Technion, Israel Institute of Technology, in 1989, 1991, and 1993 respectively. After post-doctoral research at MIT, Dr. Sapiro recently became Member of Technical Staff at the research facilities of HP Labs in Palo Alto, California.

G. Sapiro works on differential geometry and geometric partial differential equations, both in theory and applications in computer vision and image analysis.

G. Sapiro was awarded the Gutwirth Scholarship for Special Excellence in Graduate Studies in 1991, the Ollendorff Fellowship for Excellence in Vision and Image Understanding Work in 1992, and the Rothschild Fellowship for Post-Doctoral Studies in 1993.

G. Sapiro is a member of IEEE.

Albert Cohen received his Ph.D. in Mathematics from the University of Paris IX Dauphine in 1990. From 1990–1991 he held a postdoctoral position at the Bell AT&T Laboratories, New Jersey, U.S.A. Since 1995, he has been a professor in the Laboratoire d'Analyse Numerique at the Universite Pierre et Marie Curie, Paris.

He was trained in Applied Mathematics and became interested in wavelet theory when it was emerging in 1988. His first research interests were the existing relations between wavelet bases and filter banks that are used in signal and image processing. The majority of his results and publications in this domain were done in collaboration with Ingrid Daubechies at Princeton University. More recently, his area of scientific interest expanded to include approximation theory and numerical analysis.



Alfred M. Bruckstein received the B.Sc. and M.Sc. degrees in Electrical Engineering, from the Technion, Israel Institute of Technology,

in 1977 and 1980, respectively, and the Ph.D. degree in Electrical Engineering from Stanford University, Stanford, California, in 1984.

From October 1984, he has been the Technion, Haifa, Israel. He is a frequent visitor at AT&T's Bell Laboratories, Murray Hill, New Jersey (where he is presently on sabbatical). His present research interests are in Computer Vision, Pattern Recognition, Image Processing, and Computer Graphics. He has also done work in Estimation Theory, Signal Processing, Algorithmic Aspects of Inverse Scattering, Point Processes and Mathematical Models in Neurophysiology.

Prof. Bruckstein is a member of SIAM, MAA and AMS.